Enhanced memory consolidation in mice lacking the circadian modulators Sharp1 and -2 caused by elevated Igf2 signaling in the cortex

Ali Shahmoradi[a], Konstantin Radyushkin[a,2], and Moritz J. Rossner[a,b,1]

[a]Department of Neurogenetics, Max Planck Institute of Experimental Medicine, 37075 Göttingen, Germany; and [b]Department of Psychiatry, Ludwig Maximilian University, 80336 Munich, Germany

Edited by Robert C. Malenka, Stanford University School of Medicine, Stanford, CA, and approved May 21, 2015 (received for review December 15, 2014)

The bHLH transcription factors SHARP1 and SHARP2 are partially redundant modulators of the circadian system. SHARP1/DEC2 has been shown to control sleep length in humans and sleep architecture is also altered in double mutant mice ($S1/2^{-/-}$). Because of the importance of sleep for memory consolidation, we investigated the role of SHARP1 and SHARP2 in cognitive processing. $S1/2^{-/-}$ mice show enhanced cortex (Cx)-dependent remote fear memory formation as well as improved reversal learning, but do not display alterations in hippocampus (Hi)-dependent recent fear memory formation. SHARP1 and SHARP2 single null mutants do not display any cognitive phenotype supporting functional redundancy of both factors. Molecular and biochemical analyses revealed elevated insulin-related growth factor 2 (IGF2) signaling and increased phosphorylation of MAPK and S6 in the Cx but not the Hi of $S1/2^{-/-}$ mice. No changes were detected in single mutants. Moreover, adeno-associated virus type 2-mediated IGF2 overexpression in the anterior cingulate cortex enhanced remote fear memory formation and the analysis of forebrain-specific double null mutants of the Insulin and IGF1 receptors revealed their essential function for memory formation. Impaired fear memory formation in aged $S1/2^{-/-}$ mice indicates that elevated IGF2 signaling in the long term, however, has a negative impact on cognitive processing. In summary, we conclude that the bHLH transcription factors SHARP1 and SHARP2 are involved in cognitive processing by controlling *Igf2* expression and associated signaling cascades. Our analyses provide evidence that the control of sleep and memory consolidation may share common molecular mechanisms.

cortex | memory consolidation | insulin-like signaling | aging | MAPK signaling

The hippocampus (Hi) and anterior cortex (ACx) have been associated with different aspects of cognitive processes controlling, for example, recent and remote long-term fear memory formation, respectively (1). Current concepts suggest that long-term fear memory consolidation involves a gradual transfer of memory traces from hippocampal networks into stable cortical modules integrated by the anterior cingulate cortex (ACC) (2). Long-term memory consolidation is considered a highly dynamic process involving different cortical areas and is thought to be shaped already during encoding, storage, but also reconsolidation processes (3, 4). The gradual transfer of memory traces from the Hi to cortical structures is thought to be dependent on different aspects of sleep (5) such as the sleep-dependent memory replay between the Hi and the cortex (6). Thus, the controls of sleep and memory consolidation appear to be interconnected processes. It is well known that many aspects of sleep–wake-related behavior are controlled by clock genes and emerging evidence suggests an involvement of the circadian system in cognitive processes (7). Several signaling pathways have been studied in the context of hippocampal learning (8–14), among those, the circadian timing of mitogen-activated protein kinase (MAPK) activity might be important for proper memory consolidation in the hippocampus (15). Moreover, MAPK is involved in processes of long-term potentiation and memory formation (12, 16, 17). In parallel, the forebrain expressed core clock transcription factor neuronal PAS domain protein 2 (NPAS2) has been implicated in the control of nonrapid eye movement (NREM) sleep, and *Npas2*-deficient mice display deficits in hippocampus-dependent cognitive processing (18, 19). The basic loop helix (bHLH) transcription factors SHARP1 (DEC2/BHLHE41) and SHARP2 (DEC1/BHLHE40) are modulators of the circadian system and of the core clock factors circadian locomotor output cycles kaput (CLOCK) and NPAS2 and have been implicated in the control of homeostatic sleep, neuronal plasticity, and working memory (20–24). In this study, we analyzed wild type (WT), *Sharp1* and *-2* single ($S1^{-/-}$ and $S2^{-/-}$) and double knockout mice and observed exclusively in double mutants strongly enhanced cognitive performance in remote fear memory and reversal learning tasks that have been associated with the ACC and the orbitofrontal cortex as parts of the prefrontal cortex in rodents (1, 25, 26). In parallel, insulin-related growth factor 2 (IGF2) and MAPK signaling was elevated in the ACx of $S1/2^{-/-}$ mice and adeno-associated virus type 2 (AAV2)-mediated expression of *Igf2* and IGF binding protein 5 (*Igfbp5*) in the ACC caused improved and impaired remote fear memory formation in wild-type mice, respectively. Moreover, the analysis of forebrain-specific neuronal insulin receptor (*InsR*) and Igf1 receptor (*Igf1R*) double null mutant mice implicates these IGF2 responsive and MAPK signaling coupled

Significance

SHARP1 and SHARP2 transcription factors are modulators of the sleep/wake homeostasis. Sleep is thought to be important for efficient memory consolidation by gradual stabilization of hippocampus-dependent memory traces in stable cortical modules. Here, SHARP1 and SHARP2 single and double null mutant mice were investigated in cognitive processing. SHARP1 and SHARP2 double null mutants show enhanced cortex-dependent remote fear memory formation, although hippocampus-dependent recent fear memory formation is not changed. Molecular analyses revealed that insulin-related growth factor 2 (IGF2)/MAPK signaling is elevated in the cortex of double mutants and that IGF2 overexpression in the anterior cingulate cortex is sufficient to enhance fear memory consolidation. Our analyses provide evidence that the control of sleep and memory consolidation may share common molecular mechanisms.

Author contributions: A.S., K.R., and M.J.R. designed research; A.S. and K.R. performed research; A.S. and M.J.R. analyzed data; and A.S. and M.J.R. wrote the paper.

The authors declare no conflict of interest.

This article is a PNAS Direct Submission.

[1]To whom correspondence should be addressed. Email: moritz.rossner@med.uni-muenchen.de.

[2]Present address: Mouse Behavior Outcome Unit, Johannes Gutenberg University, 55128 Mainz, Germany.

This article contains supporting information online at www.pnas.org/lookup/suppl/doi:10.1073/pnas.1423989112/-/DCSupplemental.

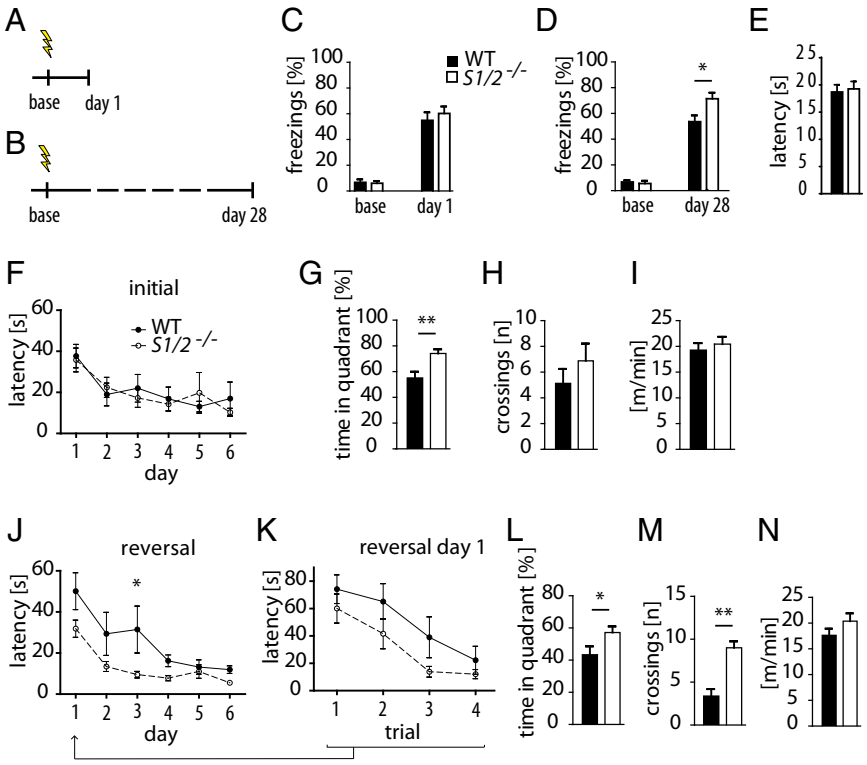

Fig. 1. Increased remote fear memory formation and improved reversal learning in $S1/2^{-/-}$ mice. (*A–E*) Experimental procedure of recent and remote memory testing upon contextual fear conditioning. (*C*) Freezing behavior of mice tested 1 d after training. No significant difference between genotypes was observed for recent fear memory. (*D*) Remote fear memory was elevated in $S1/2^{-/-}$ mice ($P < 0.05$) when tested 28 d postshock. (*E*) Hot plate experiment did not reveal any differences in nociception between the genotypes. (*F–I*) Water maze shows no difference between genotypes in the initial learning phase (*F*) but significantly increased spatial memory formation of $S1/2^{-/-}$ mice in the probe trial when monitoring the time spent in the target quadrant (*G*). The number of exact crossings of the platform location and the swim speed remained unaltered (*H* and *I*). (*J–N*) In the reversal water maze experiment (upon exchanging the position of the platform), $S1/2^{-/-}$ mice relearn to find the new platform position significantly faster compared with WT mice (*J*). The time spent in the target quadrant and the numbers of crossings of the platform location (*L* and *M*) were significantly increased in $S1/2^{-/-}$ mice compared with WT controls, indicating improved memory consolidation. Speed of swimming remained unaltered (*N*). Data shown are means ± SEM (error bars), $n = 10$ (*C*), $n =$ 12–16 (*D* and *E*), $n = 8$ (*F–N*). Statistical significance (*$P < 0.05$, **$P < 0.01$) was assessed by two-tailed Mann–Whitney *u* test (*G–I* and *L–N*) and two-way ANOVA followed by Bonferroni's post hoc test (*F*, *J*, and *K*). Effect of genotype is shown as $F_{(1,14)} = 5.76$; $P = 0.0309$ (*J*).

receptors in hippocampus- and cortex-dependent memory formation. We conclude that the circadian factors SHARP1 and -2 control aspects of cortex-dependent memory consolidation by modulating IGF2 signaling.

Results

Improved Long-Term Memory and Flexibility Learning in $S1/2^{-/-}$ Mice. To address the function of SHARP1 and SHARP2 in the context of learning and memory formation, we analyzed wild type, *Sharp1* and *Sharp2* single and double null mutants (24) in the contextual fear conditioning paradigm (27). Because of the prominent expression of *Sharp1* and *-2* in hippocampal and cortical regions and their coupling to physiologically and pathologically altered neuronal activity in the cortex (23, 28, 29), we tested recent fear memory formation (1 d after shock) to study hippocampal as well as remote fear memory (28 d after shock) to also assess cortical functions (Fig. 1 *A* and *B*). ACx regions such as the ACC appear to be critically involved in remote fear memory formation (1). $S1^{-/-}$ and $S2^{-/-}$ single mutants performed under all tested condition as WT animals (Fig. S1 *A* and *B*). $S1/2^{-/-}$ double mutants were also indistinguishable from WTs in the recent test but displayed significantly increased numbers of freezing rates in the remote test, indicating enhanced anterior cortex-dependent memory consolidation in $S1/2^{-/-}$ mice (Fig. 1 *C* and *D*). Freezing was not compromised by sensory perception as assessed by the hot plate assay where no differences between the genotypes were detected (Fig. 1*E*).

To further substantiate these findings, we applied a modified water maze task including a reversal test that monitors learning flexibility, which is also dependent on the anterior cortex (30). In the initial learning phase, performance remained unaltered during 6 d of training (Fig. 1*F*), whereas in the probe trial performed at day 7, $S1/2^{-/-}$ mice stayed significantly longer in the target quadrant but did not display increased numbers of crossings of the exact platform position, and swimming speed was unaltered between genotypes (Fig. 1 *G–I*). In contrast, after changing the platform to a new position ("reversal test") $S1/2^{-/-}$ mice relearned the task significantly faster compared with WT controls, which was already apparent on the first day of training (Fig. 1 *J* and *K*). In the reversal probe trial performed at day 14, $S1/2^{-/-}$ mice stayed significantly longer in the target quadrant and crossed the exact platform position more often (Fig. 1 *L* and *M*). Swimming speed was unaltered between genotypes (Fig. 1*N*). This observation supports the Acx-specific phenotype in $S1/2^{-/-}$ mice and indicates that improved learning and not impaired forgetting underlies the enhanced memory consolidation seen in the remote fear conditioning (Fig. 1*D*). The absence of respective phenotypes in $S1^{-/-}$ and $S2^{-/-}$ single mutants in the water maze supported the functional redundancy of both genes in cognitive processing (Fig. S1 *C–E*).

Enhanced MAPK and S6 Activity in the Anterior Cortex of *S1/2*$^{-/-}$ Mice. To further characterize the Acx-specific phenotype in *S1/2*$^{-/-}$ mice, we analyzed a set of surrogate markers of several signaling pathways (i.e., phosphorylation/activation states of p44/42-MAPK, S6, PI3K, mTOR, AMPK, GSK3β, and AKT) implicated in neuronal plasticity and hippocampal learning (8–14). We speculated that activated pathways selectively operating in the ACx and not the Hi might be among the underlying processes of the cortex-selective enhancement of learning and memory formation in *S1/2*$^{-/-}$ mice. We observed that phosphorylation of p44/42-MAPK as well as S6 in *S1/2*$^{-/-}$ mice was higher in the ACx and reduced in the Hi compared with WT controls (Fig. 1 *A–D*). This deregulation of p44/42-MAPK activity was not observed in *S1*$^{-/-}$ and *S2*$^{-/-}$ single mutants (Fig. S2). In parallel, GSK3β phosphorylation was increased in the ACx and Hi, both at a similar 1.5-fold level and we observed elevated AKT phosphorylation only in the Hi of double mutants (Fig. S3). All other signaling markers remained unaltered between the genotypes and brain regions (Fig. S3). Thus, only increased phospho-MAPK and -S6 were selectively elevated in the ACx but not the Hi of *S1/2*$^{-/-}$. We previously observed that *S1/2*$^{-/-}$ mice displayed an attenuated sleep–wake amplitude in accordance with an altered 24 activity profile by monitoring voluntary wheel running (20). Therefore, to rule out that differential physical activities and/or sleep–wake profiles might have caused differential MAPK signaling, we determined phospho-MAPK levels in 4-h bins over the complete 24-h period in the ACx and Hi of *S1/2*$^{-/-}$ and WT controls that were housed in cages equipped with running wheels. We again observed elevated phospho-MAPK levels in the ACx of *S1/2*$^{-/-}$ mice throughout the complete circadian cycle (Fig. 2 *E* and *F*), whereas genotype differences were not detectable in the Hi under these conditions (Fig. 2 *G* and *H*). We further analyzed signaling in the ACC of *S1/2*$^{-/-}$ mice by applying immunohistochemical (IHC) staining with antibodies directed against phospho-S6 before fear conditioning and directly after remote fear memory test. In agreement with published observations (31), the number of phospho-S6 positive cells increased in the ACC of WT mice upon neuronal activity, but were constitutively elevated in S1/2$^{-/-}$ mice (Fig. 2*I* and Fig. S4 *A* and *B*). We did not detect genotype differences in the CA1 region of the Hi (Fig. 2*J* and Fig. S4 *A* and *C*).

Elevated *Igf2* Expression in the Anterior Cortex of *S1/2*$^{-/-}$ Mice. Thus far, we observed an elevated level of phospho-MAPK and -S6 in the ACx that correlated with the improved anterior cortex-dependent learning performance in *S1/2*$^{-/-}$ mice. Because MAPK and S6K/S6 signaling have been shown to be coordinately activated upon growth factor and insulin signaling, we scanned available microarray data (20) at lowered significance thresholds for growth factor candidates with a differential expression in the cortex of *S1/2*$^{-/-}$ versus WT mice. The only relevant candidates identified were *Igf2* and *Igfbp5* as up- and down-regulated in *S1/2*$^{-/-}$ mice (Fig. S5). We used qRT-PCR to analyze differential mRNA expression in the ACx of *S1/2*$^{-/-}$ and WT mice over the complete circadian cycle (see above) and validated the up- and down-regulation of *Igf2* and *Igfbp5* expression, respectively, in comparison with two housekeeping genes that did not display genotype or time-dependent changes (*Rpl3a* and *Atp5b*) (Fig. 3 *A–D*). Moreover, we also validated increased *Igf2* and decreased *Igfbp5* expression in the ACx of *S1/2*$^{-/-}$ versus WT mice, normalized to the housekeeping genes (*Rpl13a* and *Cyc1*), which were unregulated (Fig. 3 *E* and *F*). No differences of genotype or time-dependent changes of *Igf2* and *Igfbp5* mRNA expression were detected in the Hi (Fig. 3*F*). Plotting the 24-h kinetics of Igf2 expression and phospho-MAPK levels obtained from WT animals only revealed their circadian profile in the ACx whereby the increase of Igf2 expression precedes the peak of MAPK activation (Fig. S6). Finally, we detected significantly elevated IGF2 protein levels in the ACx of *S1/2*$^{-/-}$ versus WT mice (Fig. 3*G*).

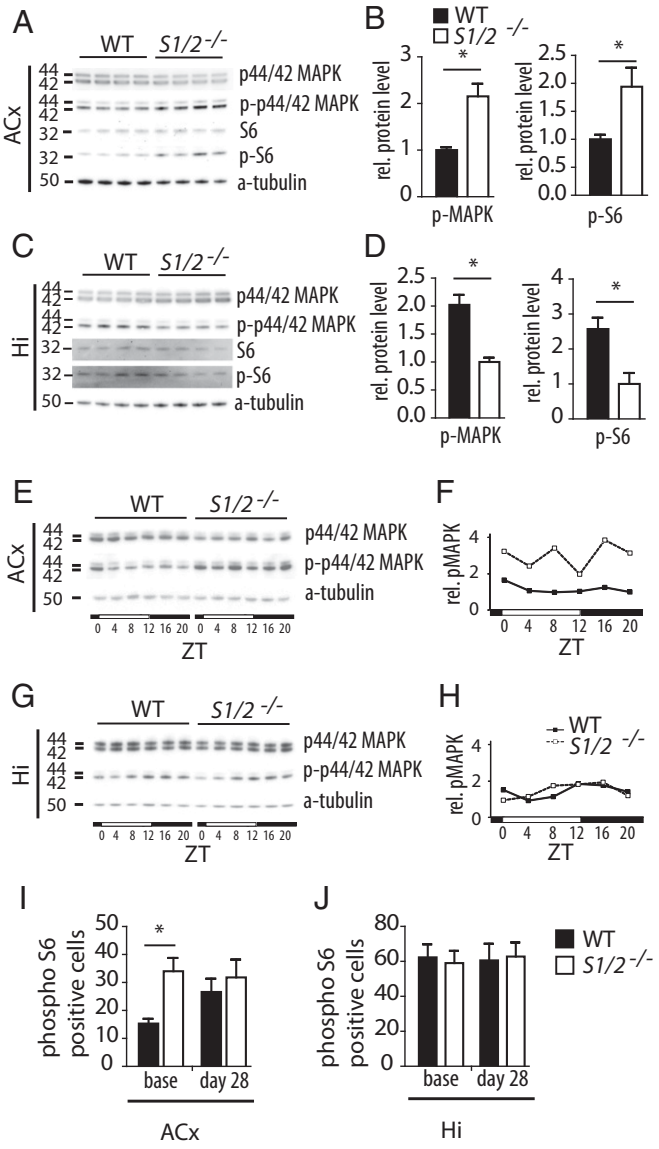

Fig. 2. Increased phosphorylation of p44/42-MAPK and S6 in the ACx of *S1/2*$^{-/-}$ mice. (*A* and *B*) Western blot analysis of ACx and Hi tissue samples obtained from WT and *S1/2*$^{-/-}$ mice. (*C* and *D*) Quantification of p44/42 MAPK and S6 phosphorylation showing an increase in MAPK and S6 phosphorylation in the ACx of *S1/2*$^{-/-}$ mice and decreased MAPK and S6 phosphorylation in the Hi compared with WT mice. (*E* and *F*) Western blot of ACx and (*G* and *H*) Hi tissue samples prepared from *S1/2*$^{-/-}$ mice housed with running wheel access showing an increase of p44/42 MAPK phosphorylation at all six time points of Zeitgeber time (ZT) over a 24-h period in the ACx (*F*), but not in the Hi (*H*). (*I* and *J*) Quantification of phospho-S6 immunohistochemistry performed with samples before fear conditioning (base) and immediately after remote memory test reveals constitutively increased number of phospho-S6 positive cells in the ACx of *S1/2*$^{-/-}$ mice independent of fear conditioning, which causes increase of phospho-S6 positive cells in WT animals. Data shown are means ± SEM (error bars), $n = 4$ (*B* and *D*), $n = 3–5$ (*I* and *J*). Statistical significance (*$P < 0.05$) was assessed by two-tailed Mann–Whitney *u* test and two-way ANOVA followed by Bonferroni's post hoc test (*F* and *H*). Effect of genotype is shown as $F_{(1,5)} = 47.83$; $P = 0.001$ (*F*).

In consequence, we hypothesized that elevating or reducing IGF2 signaling in the ACC of WT mice should enhance and inhibit remote fear memory formation, respectively. Therefore, we generated AAV2 constructs expressing *Igf2* and *Igfbp5* under the control of the CAG promoter (32) and injected corresponding viruses including an empty control virus bilaterally into

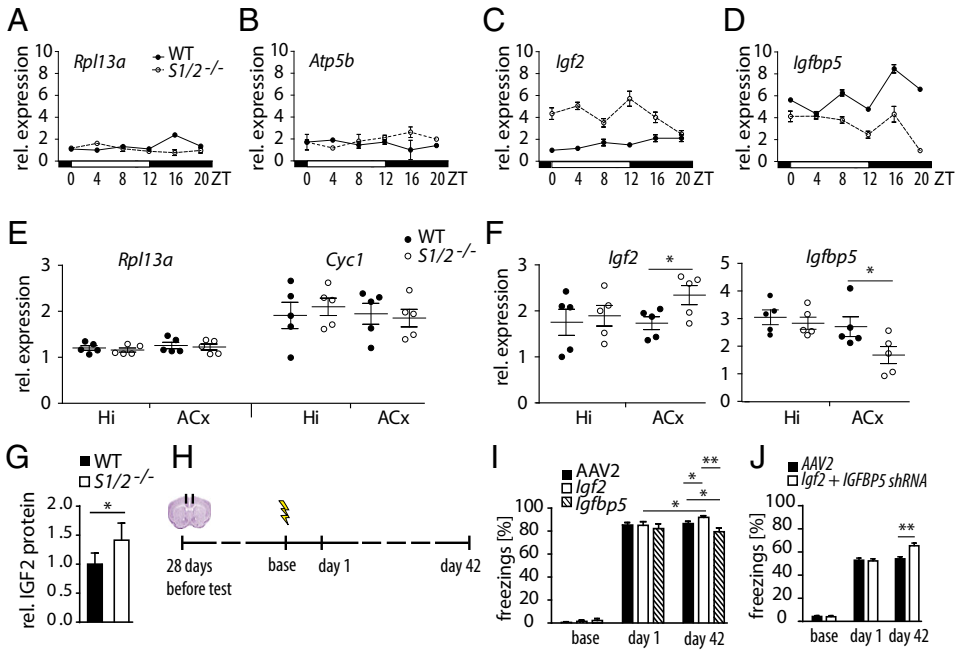

Fig. 3. Increased expression of *Igf2* and decreased *Igfbp5* expression in the ACx of *S1/2*$^{-/-}$ mice and altered remote fear memory formation by virus-mediated modulation of Igf2 signaling in the ACC of WT mice. (*A–D*) mRNA expression of ACx samples obtained at six Zeitgeber time points during 24 h from WT and S1/2$^{-/-}$ mice housed with access to running wheels. (*A* and *B*) Housekeeping genes *Rpl13a* and *Atp5b* do not display genotype or time-dependent changes. (*C*) *Igf2* mRNA expression is significantly elevated in the ACx of *S1/2*$^{-/-}$ mice compared with WT mice throughout all time points except ZT20. (*D*) The level of *Igfbp5* mRNA expression is reduced in the ACx of *S1/2*$^{-/-}$ mice compared with WT mice throughout all time points except ZT4. (*E* and *F*) RNA expression analysis in tissue samples obtained from the ACx and Hi of standard housed mice. (*E*) No genotype-dependent changes in *Rpl13a* and *Cyc1* mRNA expression in ACx and Hi of individual *S1/2*$^{-/-}$ mice compared with WT. (*F*) Increased and decreased *Igf2* and *Igfbp5* mRNA expression was detected, however, in ACx of individual *S1/2*$^{-/-}$ mice compared with WTs. No differences were observed in the Hi. (*G*) Enzyme immunoassay shows increased IGF2 protein levels in the ACx of *S1/2*$^{-/-}$ mice. Data represent normalized IGF2 levels with the average of WT values set to 1. (*H*) IGF2 and IGFBP5 encoding AAV2 viruses were introduced via stereotactic injection bilaterally into the ACC of wild-type mice 28 d prior to the fear conditioning test. Recent and remote memory was assessed 1 and 42 d after fear conditioning, respectively. (*I*) No changes in recent fear memory formation were observed 1 d after fear conditioning. In contrast, remote fear memory formation (after 42 d) was significantly enhanced and reduced by viral expression of *Igf2* and *Igfbp5*, respectively. (*J*) A pool of AAV2 viruses encoding IGF2 and expressing shRNAs targeting *Igfbp5* were introduced via bilateral stereotactic injection into the ACC of WT mice 14 d prior to the fear conditioning test. Remote memory was assessed 42 d after fear conditioning. Recent and remote memory was assessed 1 and 42 d after fear conditioning, respectively. Recent memory remained unchanged, whereas remote fear memory was significantly elevated upon coexpression of Igf2- and Igfbp5-directed shRNAs. Data shown are means ± SEM (error bars), $n = 5$ (*E* and *F*), $n = 4$ (*G*), $n = 7$–19 (*I*), $n = 15$–16 (*J*). Statistical significance (*$P < 0.05$, **$P < 0.01$) was assessed by two-tailed Mann–Whitney *u* (*F*, *I*, and *J*), two-way ANOVA followed by Bonferroni's post hoc test (*A–D*), and unpaired *t* test (*G*). Effect of genotype is shown as $F_{(1,5)} = 18.47$; $P = 0.0077$ (*C*) and $F_{(1,5)} = 12.07$; $P = 0.0178$ (*D*).

the ACC of WT mice (Fig. 3*H*). Four weeks after injection and recovery, animals were subjected to fear conditioning and were analyzed for recent and remote memory formation. Mice with virus-mediated overexpression of *Igf2* in the ACC displayed a slight yet significant improvement of remote fear memory formation ($P < 0.05$) (Fig. 3*I*). In contrast, animals that were injected with an *Igfbp5*-encoding virus showed a significantly impaired remote fear memory formation compared with the control ($P < 0.05$) and to Igf2 injections ($P < 0.01$) (Fig. 3*I*). To better reflect the situation in *S1/2*$^{-/-}$ mice, where *Igf2* expression is elevated and *Igfbp5* expression is reduced in the ACx (Fig. 2 *A–G*), we coinjected a pool of AAV2 constructs coding both for IGF2 and those expressing shRNAs directed against *Igfbp5* bilaterally into the ACC and assessed recent and remote fear memory. The simultaneous increase of IGF2 and decrease of the insulin-signaling inhibitor IGFBP5 resulted in a highly significant enhancement of remote fear memory ($P < 0.001$) (Fig. 3*J*). Modulation of IGF2 signaling by virus-mediated *Igf2*/*Igfbp5* expression in the ACC did not affect hippocampus-dependent recent fear memory (Fig. 3 *I* and *J*).

Redundant Function of INSR and IGF1R in the Forebrain Is Associated with Reduced MAPK Signaling in the ACx but Not the Hi. The canonical receptors that are known to bind insulin-like peptides including IGF2 are the INSR and IGF1R, which both mediate downstream signaling via the ERK/MAPK pathway (33). When inactivated individually, however, deficits in learning and memory formation have not been described so far (34, 35). Therefore, we generated forebrain-specific neuronal *InsR* and *Igf1R* double null mutant mice by crossing *Igf1R*/*InsR*$^{fl/fl}$ mice (36, 37) with *CaMKII-cre*–expressing mice (38) to study consequences on MAPK signaling and fear memory formation. As expected by the expression pattern of CaMKII, INSR and IGF1R protein levels were highly reduced in the ACx (Fig. 4 *A* and *B*) and Hi (Fig. 4 *D* and *E*) in *Igf1R*/*InsR*$^{CaMKII\text{-}cre}$ compared with *Igf1R*/*InsR*$^{fl/fl}$ mice. Phosphorylation levels of p44/42-MAPK were, however, significantly reduced only in the ACx (Fig. 4*C*) but not in the Hi (Fig. 4*D*) of the double mutants. We subsequently subjected *Igf1R*/*InsR*$^{fl/fl}$ and *Igf1R*/*InsR*$^{CaMKII\text{-}cre}$ mice to a series of standard behavioral tests and did not observe any altered behavior among both groups (Fig. S7). Thus, forebrain restricted deletion of the INSR and IGF1R in *CaMKII* positive neurons does not alter basic behavior. We next used the contextual fear conditioning paradigm and analyzed recent and remote memory formation (Fig. 4*G*). *Igf1R*/*InsR*$^{CaMKII\text{-}cre}$ mice displayed a highly significant impaired recent and remote fear memory performance compared with the controls (Fig. 4*H*). As it was shown before for neuronal *InsR* knockout mice under high fat diet, the double

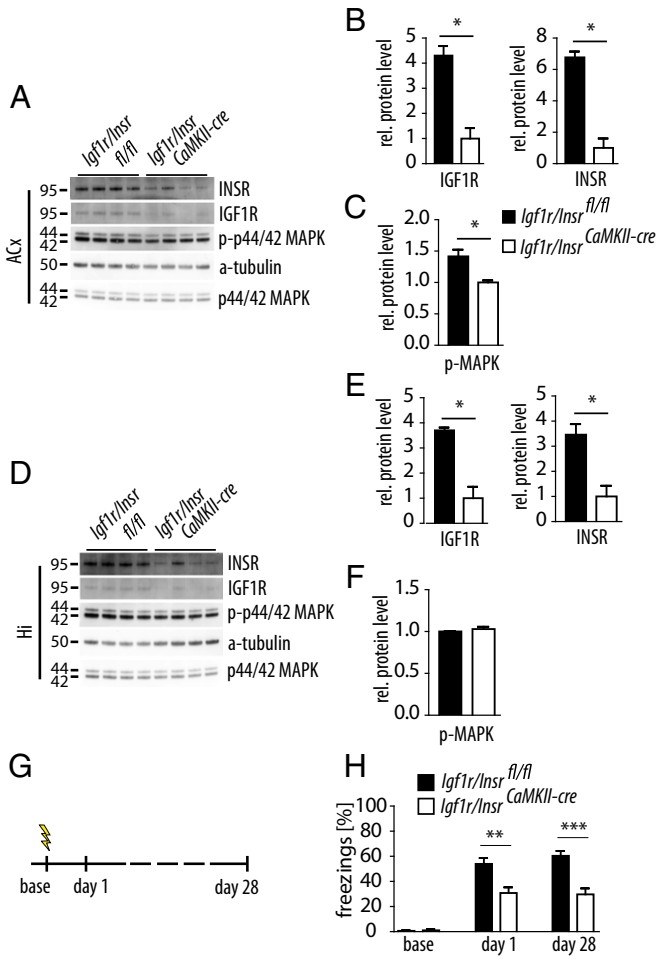

Fig. 4. Neuronal knockout of *InsR* and *Igf1R* in the cortex and hippocampus impairs fear learning and MAPK signaling in the ACx. (*A* and *D*) Western blots of samples obtained from the ACx and Hi of *Igf1R/InsR*$^{fl/fl}$ and *Igf1R/InsR*$^{CaMKII\text{-}cre}$ mice. (*B*, *C*, *E*, and *F*) Quantification of Western blot data showing reduced phosphorylation of MAPK in the ACx but not the Hi. (*G* and *H*) *Igf1R/InsR*$^{CaMKII\text{-}cre}$ display highly significantly reduced fear learning compared with *Igf1R/InsR*$^{fl/fl}$ control mice 1 d and 28 d after conditioning. Data shown are means ± SEM (error bars), $n = 4$ (*A*–*F*), $n = 13$–17 (*G* and *H*). Statistical significance (*$P < 0.05$, **$P < 0.01$, ***$P < 0.005$) was assessed by two-tailed Mann–Whitney *u* test.

knockout mice displayed a significant gain of weight already under standard diet (Fig. S8), which has been attributed to reduced insulin signaling (39). These data reveal that INSR and IGF1R are at least partially redundant in the forebrain and the loss of both receptors impairs MAPK signaling in the ACx but not the Hi. In addition, our observations indirectly support the implication of the IGF2-IGF1R/INSR-MAPK signaling axis for memory consolidation in the cortex.

Impaired Fear Memory Formation in Aged *S1/2*$^{-/-}$ Mutant Mice. To understand the long-term effects of SHARP1 and SHARP2 deficiency caused by enhanced *Igf2* signaling, we studied aging *S1/2*$^{-/-}$ mice and observed an age-dependent weight loss and increased mortality rate in aged *S1/2*$^{-/-}$ mice (Fig. 5 *A* and *B*). Whereas *Igf2* expression remained elevated in the ACx and unchanged in the Hi, expression levels of *Igfbp5* were similar in the ACx and Hi of aged *S1/2*$^{-/-}$ and WT mice (Fig. 5*D*). The phosphorylation of p44/42-MAPK in the ACx of *S1/2*$^{-/-}$ mice was reduced to WT levels (Fig. 5 *F* and *G*) and remained reduced in the Hi of *S1/2*$^{-/-}$ mice (Fig. 5 *H* and *I*). In parallel, the overall performance of *S1/2*$^{-/-}$ mice in contextual fear conditioning was significantly reduced in the recent and reduced to wild-type levels in the remote task (Fig. 5 *J* and *K*).

Discussion

Long-term memory consolidation such as remote fear memory formation is thought to depend on the gradual transfer of memory traces from hippocampal to cortical structures in a periodic and sleep-dependent process, which may involve the function of clock genes (40). In this study, we analyzed cognitive processing in single and double null mouse mutants of the clock modulators SHARP1 and -2. We discovered that *S1/2*$^{-/-}$ mice display enhanced performance in cortex-dependent learning tasks, which is paralleled by elevated *Igf2* expression and MAPK signaling in the ACx but not the Hi. Moreover, virally modulated IGF2 signaling in the ACC altered remote fear memory formation in WT mice. We conclude that elevated IGF2 expression in the ACx might activate MAPK signaling to enhance memory consolidation in cortex-dependent learning tasks in *S1/2*$^{-/-}$ mice. MAPK signaling has already been reported to be important for hippocampal memory formation in mice (12) and in long-term memory consolidation in *Aplysia californica* (17, 41) and the crab *Chasmagnathus* (42). Moreover, MAPK signaling has been associated with circadian aspects of hippocampal memory formation, although the upstream mechanisms have not yet been identified so far (15). In addition, IGF2 signaling has been associated with memory consolidation and extinction of fear memory in the hippocampus (34, 43, 44). Our analysis reveals an additional role for IGF2/MAPK signaling in cortex-dependent cognitive processing. MAPK as well as S6 signaling are known to be targeted by Igf2 and insulin signaling through the insulin and Igf1 receptor (45, 46). Inactivation of the INSR does not exhibit a substantial change in learning or memory abilities of mice (34, 35), and inhibition of the IGF1R has no impact on fear memory (34), which might be explained by a functional redundancy among these structurally highly related receptors. We proved this hypothesis in mice with conditional forebrain-specific double *InsR* and *Igf1R* null mutants that exhibited a highly reduced memory formation. An associated reduction of MAPK activity in *Igf1R/InsR*$^{CaMKII\text{-}cre}$ compared with *Igf1R/InsR*$^{fl/fl}$ mice, however, was restricted to the ACx and could not be observed in the Hi. Therefore, it seems likely that IGF2 signaling uses regionally different modes of action using both the IGF1R/INSR and IGF2R to activate MAPK in a context-dependent way (34, 43, 44, 47). The significance of MAPK activity for the timing of memory formation in the hippocampus has been addressed already in a circadian context (15, 17, 41) and the disruption of clock genes leads to a memory impairment (48–51). Because circadian and activity-coupled mRNA expression of *Sharp1/2* is restricted to the cortex (23, 28), it appears likely that in the corresponding mouse mutant cortex-selective processes are affected. We could show that *Igf2* expression and MAPK activation display a circadian regulation in the cortex of WT mice that appears to be uncoupled upon loss of the negative clock modulators SHARP1/2. Our study thus paves the way to investigate circadian and sleep-associated aspects of cortex-dependent memory consolidation in more depth in the future. Moreover, our analysis supports the hypothesis that the control of sleep and memory consolidation may be controlled by similar mechanisms including IGF2-dependent signaling. IGF2 seems to be a potent memory enhancer in the hippocampus (34, 43, 52) as well as in the cortex (our study) and factors of insulin-like signaling are under investigation as putative therapeutical agents to overcome cognitive decline upon aging and in neurodegenerative and psychiatric disease conditions (53–57). Recently, we could show that *S1/2*$^{-/-}$ mice display an impaired working memory (20), whereas long-term memory consolidation is enhanced (this study), which may be explained by the fact that the

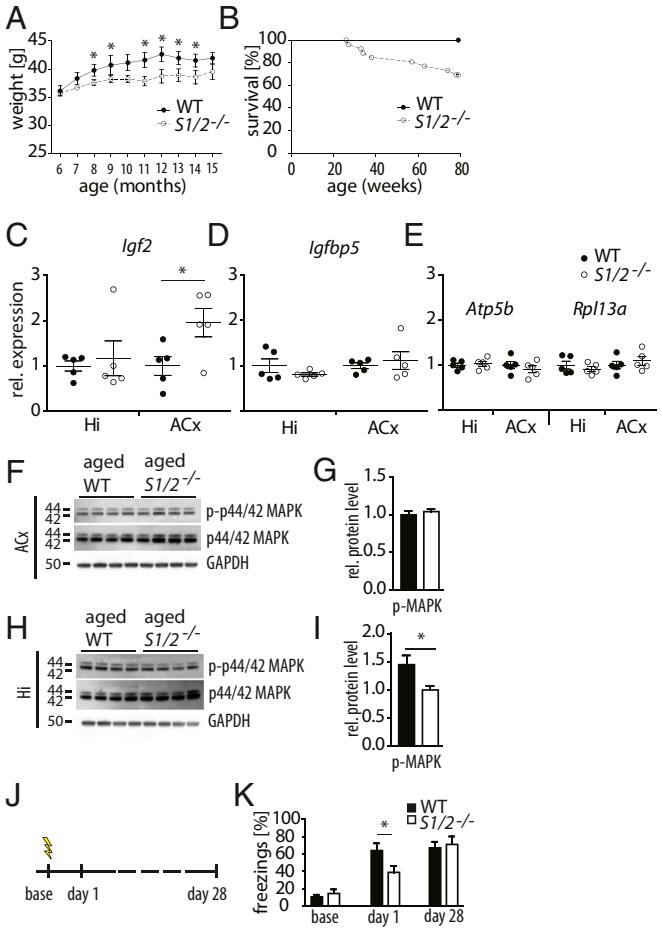

Fig. 5. Reduced life span and cognitive decline of aged *S1/2*$^{-/-}$ mice. (*A* and *B*) Weight analyses and survival curve showing reduced weight (*A*) and decreased life span (*B*) of aged *S1/2*$^{-/-}$ double knockout mice compared with wild-type mice. (*C*–*E*) RNA expression analyses showing increased *Igf2* RNA expression in the ACC, but not Hi, and unaltered *Igfbp5* expression in both regions. (*F* and *H*) Western blot analyses of ACx and Hi samples from aged *S1/2*$^{-/-}$ and WT mice. (*G* and *I*) Quantification of Western blot data, showing unaltered MAPK phosphorylation in the ACx and decreased MAPK phosphorylation in the Hi of *S1/2*$^{-/-}$ mice compared with WT mice. (*J* and *K*) Fear conditioning experiment with memory test 1 d and 28 d after conditioning, showing reduced recent memory of *S1/2*$^{-/-}$ compared with WT mice at day 1 after conditioning and remote fear memory (day 28) reduced to levels of WT animals in contrast to young adult mice (Fig. 1*D*). Data shown are means ± SEM (error bars), $n = 13$–14 (*A*), $n = 26$–30 (*B*), $n = 5$ (*C*–*E*), $n = 4$ (*F* and *I*), $n = 10$–12 (*J* and *K*). Statistical significance (*$P < 0.05$) was assessed by two-tailed Mann–Whitney *u* test, Gehan–Breslow–Wilcoxon test (*B*), and two-way ANOVA followed by Bonferroni's post hoc test (*A*). Effect of genotype is shown as $F_{(1,25)} = 3.51$; $P = 0.0729$ (*A*).

underlying principles of both systems are fundamentally different and are most likely differentially affected in S1/2$^{-/-}$ mice. In addition, aged S1/2$^{-/-}$ mice, however, display a strong decline in memory performance. Although it is not clear whether this effect is mediated by the lack of additional functions of SHARP1/2 or continuously increased levels of *Igf2* expression, it seems imperative to better understand the long-term consequences of elevated IGF2 on the neuronal metabolism and aging-related processes that may not only provide beneficial effects as memory enhancer.

Materials and Methods

Animal Experiments. All animal experiments were performed in accordance with Regierungspräsidium Braunschweig institutional guidelines and were approved by the government of Lower Saxony, Germany.

Mice were housed at a 12-h light/12-h dark cycle and received food and water available ad libitum. All experiments were performed with cohorts of adult male mice at the same age between 4–5 mo and 12–16 mo for aging studies. *S1*$^{-/-}$, *S2*$^{-/-}$, *Igf1R*$^{fl/fl}$, and *InsR*$^{fl/fl}$ single knockout mice as well as *CaMKII-cre* heterozygous mice were backcrossed to C57BL/6J for more than 10 generations as described previously (24, 36–38). WT and *Sharp1* and *-2* double mutant mice (*S1/2*$^{-/-}$) were obtained from double heterozygous breeding pairs (24, 58). *Igf1R/InsR*$^{fl/fl}$ and *Igf1R/InsR*$^{CaMKII\text{-}cre}$ mice were obtained from *Igf1R/InsR*$^{fl/fl}$ homozygous and *CaMKII-cre* heterozygous breeding pairs. *Igf1R/InsR*$^{fl/fl}$ homozygous mice were obtained from Igf1R/InsR$^{fl/+}$ heterozygous breeding pairs. *Igf1R/InsR*$^{fl/+}$ heterozygous mice were obtained from *Igf1R*$^{fl/fl}$ and *InsR*$^{fl/fl}$ breeding pairs. All experiments were performed blinded to genotypes.

Stereotactic Injections. Surgery was performed under intraperitoneal anesthesia with ketamine/xylazine (100 mg/kg; 10 mg/kg). Viral vectors (AAV2, AAV2-*Igf2*, AAV2-*Igfbp5*, or a pool of AAV2-*Igf2/Igfbp5shRNA1-3*) were injected into the anterior cingulate cortex (1 mm anterior to bregma, 0.5 mm lateral to midline, 1.5 mm ventral to surface). One microliter was administered at each injection site using a 10-μL Hamilton syringe at a rate of 0.5 μL/min with a total of 2–4 × 10^{11} virus particles per injection site. Immediately after surgery, mice were given buprenorphine (0.2 mg/kg, s.c.) for analgesia.

Western Blot Analyses. Brain tissues (ACx bregma 1–3 mm and Hi bregma −1 to −3 mm) were isolated using a "rodent brain matrix" 1 mm coronal slicer (ASI Instruments) from adult WT and S1/2$^{-/-}$ mice harvested at indicated time points. ACx and Hi samples were frozen on dry ice and lysed with a Polytron PT 2000 homogenizer in sucrose buffer. Samples obtained at defined Zeitgeber time points were collected as described above and pooled ($n = 3$). For preservation of proteins as well as of protein phosphorylation cOmplete (Roche) and PhosSTOP tablets were freshly added to the buffer. After lysis of the tissue, a fraction of the lysate was removed and added to an appropriate volume of RNA lysis buffer (Qiagen) for further RNA extraction. Protein lysates were quantified with a Lowry-based DC Protein Assay Kit II (Bio-Rad) and added to a final concentration of 1 mM DTT and 1× NuPAGE lithium dodecyl sulfate (LDS) sample buffer. Samples were heated for 10 min at 70 °C and separated in 4–12% NuPAGE Bis-Tris gel/1× Mes buffer (Invitrogen). Protein was transferred to a 0.2-μm PVDF membrane (Roche) and blocked overnight in 5% milk in 1× TBS with 0.05% Tween 20. Immunoblots were visualized with HRP-coupled secondary antibodies and an INTAS ECL Imager.

Enzyme Immunoassay. Detection of IGF2 protein levels in ACx homogenates from *S1/2*$^{-/-}$ and WT mice was essentially performed as described (59) with minor modifications. Protein extracts were concentrated using Amicon Ultra filter units (Millipore) and IGF2 levels were determined following the instructions provided by the manufacturer's protocol (Abcam) and absorbance was measured using a 96-well microtiter plate reader (Berthold) against a standard curve obtained from serial dilutions of recombinant human IGF2 (R&D Systems).

Plasmids. ORF-containing expression cassettes encoding mouse IGF2 and IGFBP5 were synthesized using gene blocks (Integrated DNA Systems) and subcloned into an AAV2 plasmid backbone containing a CAG promoter (obtained from M. Klugmann, University of New South Wales, Australia) Three hairpin shRNAs constructs targeting Igfbp5 mRNA (NM_010518.2) were designed using an online tool available at cancan.cshl.edu/RNAi_central using standard settings, synthesized as oligonucleotides, and subcloned into the same AAV2-CAG backbone as follows: shRNA1: TGCTGTTGACAGTGAGCG-CAGACTTTATAGGCATATAAAT TAGTGAAGCCACAGATGTAATTTATATGCCTAT-AAAGTCTATGCCTACTGCCTCGGA; shRNA2: TGCTGTTGACAGTGAGCGATCTCT-TGATGGCATGGCATAG TAGTGAAGCCACAGATGTACTATGCCATGCCATCAAGA-GAGTGCCTACTGCCTCGGA; and shRNA3: TGCTGTTGACAGTGAGCGCCCTCTGG-CTTTCAAGAGAAAG TAGTGAAGCCACAGATGTACTTTCTCTTGAAAGCCAGAGGA-TGCCTACTGCCTCGGA.

The Igfbp5 targeting sequence is underlined.

Quantification of shRNA constructs was performed with qRT-PCR on cDNA obtained from mouse NIH 3T3 cells nucleofected with AAV2, AAV2-*Igfbp2*-shRNA1, AAV2-*Igfbp2*-shRNA2, AAV2-*Igfbp2*-shRNA3, and a pool of AAV2-*Igfbp2*-shRNA1–3 plasmid constructs performed in triplicates. Transfection efficiency was determined to be higher than 70%. Knockdown efficiency in reference to the AAV2 control was 32 ± 6% for shRNA1, 43 ± 9% for shRNA2, 39 ± 4% for shRNA2, and 65 ± 7% for a pool of shRNAs1–3. Therefore, a mix of AAV2-*Igfbp5*-shRNA1–3 plasmids was used for virus generation and injection in a pool with AAV2-*Igf2*.

Antibodies. The following antibodies were used in our experiments: AKT (1:2,000; Cell Signaling), phospho-AKT (1:2,000; Cell Signaling), AMPK (1:1,000; Cell Signaling), phospho-AMPK (1:1,000; Cell Signaling), GAPDH (1:500; Stressgen), GSK3β (1:2,000; Cell Signaling), phospho-GSK3β (1:2,000; Cell Signaling), IGF1R (1:1,000; Cell Signaling), INSR (1:1,000; Cell Signaling), p44/42-MAPK (1:2,000; Cell Signaling), phospho-p44/42-MAPK (1:2,000; Cell Signaling), mTOR(1:1,000; Cell Signaling), phospho-mTOR (1:1,000; Cell Signaling), PI3K (1:1,000; Cell Signaling), phospho-PI3K (1:1,000; Cell Signaling), S6 (1:1,000; Cell Signaling), phospho-S6 (1:1,000; Cell Signaling), and α-tubulin (1:10,000; Sigma).

RNA Expression Analyses. RNA was isolated according to the manufacturer's manual using RNeasy columns (Qiagen). All isolated RNA samples were tested for quality and quantity with the Bioanalyzer (Agilent Technologies). RNA-integrity (RIN) values were higher than 8. SYBRgreen real-time PCR experiment was performed with a LC480 detection system (Roche). All primers were designed online at the assay design center of the Roche Universal Probe Library: *Atp5b* (S:GGATCTGCTGGCCCCATAC, AS:CTTTCCAACGCCAGCACCT), *Cyc1* (S:CAGAGCATGACCATCGAAAA, AS:CACTTATGCCGCTTCATGG), *Igf2* (S:CGCTTCAGTTTGTCTGTTCG, AS:GCAGCACTCTTCCACGATG), *Igfbp5* (S:CTACCGCGAGCAAGTCAAG, AS:GTCTCCTCGGCCATCTCA), and *Rpl13a* (S:ATCCCTCCACCCTATGACAA, AS:GCCCCAGGTAAGCAAACTT).

Immunostainings. Mice were anesthetized with avertin and perfused with gassed ACSF following 4% (wt/vol) PFA in PBS. Then, brains were treated overnight in 4% PFA at 4 °C and embedded in paraffin. Immunohistochemical analysis was performed on 10-μm-thick coronal brain sections. Hematoxylin-eosin (H&E) stain as well as a DAB-based immunostaining Dako-LSAB2 kit was used according to the manufacturer's manual. Primary antibody was used against phospho-S6 (1:100; Cell Signaling). For quantification, cells were counted within a defined identical square, whereas only cells were counted that were completely in the square.

Behavioral Analyses. Behavioral tests were performed as described (60) with minor modifications. In short, to test anxiety behavior, the light–dark preference test was performed in a box consisting of two equal parts, a dark and a transparent compartment connected by a door. Within 5 min, time spent in the dark was analyzed. The spontaneous locomotor activity of mice was tested in the open field test. Test time for each animal was 10 min. In this time, the total time active, the number of rearing, the total time of rearing, traveled distance, time at the center and the periphery, and corner visits were analyzed. The setup was modified for the hole board test by changing the floor to a plastic plate with 16 symmetrical holes. Within 10 min, the traveled distance, the number of visits at the holes, the total exploration time, as well as the time spent for one exploration was measured and analyzed. To test the pain threshold with the hot plate test, each mouse was placed on a 52 °C metal plate, and the time until the mice licked the hind paw was measured. To test the overall motivation behavior of mice, a tail suspension test was performed. For this purpose, mice hung on their tails for 6 min and the time of struggling to get free was measured. To test the anxiety behavior, mice were tested in an elevated plus maze test. The test setup has two open arms and two closed arms, and preference of mice was tested. Test duration was 5 min, during which total distance traveled, distance traveled in closed arms, time spent in center, running speed, and relative time in closed arms were analyzed. Spatial learning and memory were analyzed in the Morris water maze test. The test started with a 2-d visible platform task to allow the mice to learn the platform position. For initial and reversal learning the flag was removed from the platform. During the following 6 d of spatial learning (initial learning) each mouse was released in the tank four times per day and allowed to swim until it found the hidden platform. After 6 d, a probe trial was performed to access the memory of the mice by removing the platform and measuring the time spent in the target quadrant, number of crossings of the platform position, and swim speed. After a 7-d break, the reversal learning test was performed. The hidden platform was placed in the opposite quadrant and learning was assessed for 6 d. Finally, the reversal probe trial was performed to assess memory formation. Contextual fear memory was assessed in fear conditioning paradigm with several cohorts of mice. All cohorts were tested with TSE Systems equipment, with 0.4-mA shock intensity and 2-s duration. AAV2-injected mice were tested with a Ugo Basile system. Parameters for shock intensity and duration (0.4 mA, 2 s) were identical for AAV2, AAV2-*IGF2*, and AAV2-*IGFBP5* injections. Duration was reduced to 1 s for AAV2 and AAV2-*IGF2*/*IGFBP5*-shRNA coinjections to avoid ceiling effects. The freezing rate of the AAV-injected mice was analyzed automatically by Any Maze software (Stoelting). Animals for immunohistochemical analyses were killed before conditioning (baseline) and 28 d after conditioning, respectively. More specific information on behavioral experiments was described previously (60).

Aging Cohort. Weight was noted every month from 6 to 15 mo of age. Genotype differences in the survival curve until the age of 80 wk were analyzed statistically with the Gehan–Breslow–Wilcoxon test.

Protein and RNA Quantification. Western blot signal intensities were quantified with ImageJ software. Phosphorylation-specific antibodies were normalized with respective pan antibodies to the total amount of the studied protein. Other protein signals were quantified to tubulin. Real-time PCR signals were normalized to two housekeeping genes out of *Atp5b*, *Cyc1*, and *Rpl13a*, respectively.

ACKNOWLEDGMENTS. We thank K.-A. Nave for continuous support, L. Reinecke and M. M. Brzózka for support with behavioral experiments, and R. Taneja and J. C. Brüning for providing transgenic mice. This work was supported by Grants RO 4076/3-1 and RO 4076/5-1 from the Deutsche Forschungsgemeinschaft (to M.J.R.).

1. Frankland PW, Bontempi B, Talton LE, Kaczmarek L, Silva AJ (2004) The involvement of the anterior cingulate cortex in remote contextual fear memory. *Science* 304(5672): 881–883.
2. Frankland PW, Bontempi B (2005) The organization of recent and remote memories. *Nat Rev Neurosci* 6(2):119–130.
3. Dudai Y, Morris RGM (2013) Memorable trends. *Neuron* 80(3):742–750.
4. Wang S-H, Morris RGM (2010) Hippocampal-neocortical interactions in memory formation, consolidation, and reconsolidation. *Annu Rev Psychol* 61:49–79, C1–4.
5. Diekelmann S, Born J (2010) The memory function of sleep. *Nat Rev Neurosci* 11(2): 114–126.
6. Ji D, Wilson MA (2007) Coordinated memory replay in the visual cortex and hippocampus during sleep. *Nat Neurosci* 10(1):100–107.
7. Eckel-Mahan KL, Storm DR (2009) Circadian rhythms and memory: Not so simple as cogs and gears. *EMBO Rep* 10(6):584–591.
8. Bekinschtein P, et al. (2007) mTOR signaling in the hippocampus is necessary for memory formation. *Neurobiol Learn Mem* 87(2):303–307.
9. Chen X, et al. (2005) PI3 kinase signaling is required for retrieval and extinction of contextual memory. *Nat Neurosci* 8(7):925–931.
10. Enriquez-Barreto L, et al. (2014) Learning improvement after PI3K activation correlates with de novo formation of functional small spines. *Front Mol Neurosci* 6.
11. Fortress AM, Schram SL, Tuscher JJ, Frick KM (2013) Canonical Wnt signaling is necessary for object recognition memory consolidation. *J Neurosci* 33(31): 12619–12626.
12. Kelleher RJ, 3rd, Govindarajan A, Jung H-Y, Kang H, Tonegawa S (2004) Translational control by MAPK signaling in long-term synaptic plasticity and memory. *Cell* 116(3): 467–479.
13. Man H-Y, et al. (2003) Activation of PI3-kinase is required for AMPA receptor insertion during LTP of mEPSCs in cultured hippocampal neurons. *Neuron* 38(4):611–624.
14. Potter WB, et al. (2010) Metabolic regulation of neuronal plasticity by the energy sensor AMPK. *PLoS ONE* 5(2):e8996.
15. Eckel-Mahan KL, et al. (2008) Circadian oscillation of hippocampal MAPK activity and cAmp: Implications for memory persistence. *Nat Neurosci* 11(9):1074–1082.
16. Orban PC, Chapman PF, Brambilla R (1999) Is the Ras-MAPK signalling pathway necessary for long-term memory formation? *Trends Neurosci* 22(1):38–44.
17. Philips GT, Ye X, Kopec AM, Carew TJ (2013) MAPK establishes a molecular context that defines effective training patterns for long-term memory formation. *J Neurosci* 33(17):7565–7573.
18. Franken P, Dijk D-J (2009) Circadian clock genes and sleep homeostasis. *Eur J Neurosci* 29(9):1820–1829.
19. Reick M, Garcia JA, Dudley C, McKnight SL (2001) NPAS2: An analog of clock operative in the mammalian forebrain. *Science* 293(5529):506–509.
20. Baier PC, et al. (2014) Mice lacking the circadian modulators SHARP1 and SHARP2 display altered sleep and mixed state endophenotypes of psychiatric disorders. *PLoS ONE* 9(10):e110310.
21. He Y, et al. (2009) The transcriptional repressor DEC2 regulates sleep length in mammals. *Science* 325(5942):866–870.
22. Pruunsild P, Sepp M, Orav E, Koppel I, Timmusk T (2011) Identification of cis-elements and transcription factors regulating neuronal activity-dependent transcription of human BDNF gene. *J Neurosci* 31(9):3295–3308.
23. Rossner MJ, Dörr J, Gass P, Schwab MH, Nave KA (1997) SHARPs: Mammalian enhancer-of-split- and hairy-related proteins coupled to neuronal stimulation. *Mol Cell Neurosci* 10(3-4):460–475.
24. Rossner MJ, et al. (2008) Disturbed clockwork resetting in Sharp-1 and Sharp-2 single and double mutant mice. *PLoS ONE* 3(7):e2762.
25. Bissonette GB, Powell EM (2012) Reversal learning and attentional set-shifting in mice. *Neuropharmacology* 62(3):1168–1174.

26. McAlonan K, Brown VJ (2003) Orbital prefrontal cortex mediates reversal learning and not attentional set shifting in the rat. *Behav Brain Res* 146(1-2):97–103.
27. Kim JJ, Fanselow MS (1992) Modality-specific retrograde amnesia of fear. *Science* 256(5057):675–677.
28. Honma S, et al. (2002) Dec1 and Dec2 are regulators of the mammalian molecular clock. *Nature* 419(6909):841–844.
29. Li JZ, et al. (2013) Circadian patterns of gene expression in the human brain and disruption in major depressive disorder. *Proc Natl Acad Sci USA* 110(24):9950–9955.
30. de Bruin JP, Sànchez-Santed F, Heinsbroek RP, Donker A, Postmes P (1994) A behavioural analysis of rats with damage to the medial prefrontal cortex using the Morris water maze: Evidence for behavioural flexibility, but not for impaired spatial navigation. *Brain Res* 652(2):323–333.
31. Knight ZA, et al. (2012) Molecular profiling of activated neurons by phosphorylated ribosome capture. *Cell* 151(5):1126–1137.
32. Niwa H, Yamamura K, Miyazaki J (1991) Efficient selection for high-expression transfectants with a novel eukaryotic vector. *Gene* 108(2):193–199.
33. Siddle K (2011) Signalling by insulin and IGF receptors: Supporting acts and new players. *J Mol Endocrinol* 47(1):R1–R10.
34. Chen DY, et al. (2011) A critical role for IGF-II in memory consolidation and enhancement. *Nature* 469(7331):491–497.
35. Schubert M, et al. (2004) Role for neuronal insulin resistance in neurodegenerative diseases. *Proc Natl Acad Sci USA* 101(9):3100–3105.
36. Brüning JC, et al. (1998) A muscle-specific insulin receptor knockout exhibits features of the metabolic syndrome of NIDDM without altering glucose tolerance. *Mol Cell* 2(5):559–569.
37. Klöting N, et al. (2008) Autocrine IGF-1 action in adipocytes controls systemic IGF-1 concentrations and growth. *Diabetes* 57(8):2074–2082.
38. Minichiello L, et al. (1999) Essential role for TrkB receptors in hippocampus-mediated learning. *Neuron* 24(2):401–414.
39. Brüning JC, et al. (2000) Role of brain insulin receptor in control of body weight and reproduction. *Science* 289(5487):2122–2125.
40. Gerstner JR, Yin JCP (2010) Circadian rhythms and memory formation. *Nat Rev Neurosci* 11(8):577–588.
41. Philips GT, Tzvetkova EI, Carew TJ (2007) Transient mitogen-activated protein kinase activation is confined to a narrow temporal window required for the induction of two-trial long-term memory in Aplysia. *J Neurosci* 27(50):13701–13705.
42. Feld M, Dimant B, Delorenzi A, Coso O, Romano A (2005) Phosphorylation of extranuclear ERK/MAPK is required for long-term memory consolidation in the crab Chasmagnathus. *Behav Brain Res* 158(2):251–261.
43. Agis-Balboa RC, et al. (2011) A hippocampal insulin-growth factor 2 pathway regulates the extinction of fear memories. *EMBO J* 30(19):4071–4083.
44. Iwamoto T, Ouchi Y (2014) Emerging evidence of insulin-like growth factor 2 as a memory enhancer: A unique animal model of cognitive dysfunction with impaired adult neurogenesis. *Rev Neurosci* 25(4):559–574.
45. Hu Q, et al. (2011) Wt1 ablation and Igf2 upregulation in mice result in Wilms tumors with elevated ERK1/2 phosphorylation. *J Clin Invest* 121(1):174–183.
46. Roux PP, et al. (2007) RAS/ERK signaling promotes site-specific ribosomal protein S6 phosphorylation via RSK and stimulates cap-dependent translation. *J Biol Chem* 282(19):14056–14064.
47. Schmeisser MJ, et al. (2012) IκB kinase/nuclear factor κB-dependent insulin-like growth factor 2 (Igf2) expression regulates synapse formation and spine maturation via Igf2 receptor signaling. *J Neurosci* 32(16):5688–5703.
48. Kondratova AA, Dubrovsky YV, Antoch MP, Kondratov RV (2010) Circadian clock proteins control adaptation to novel environment and memory formation. *Aging (Albany, NY Online)* 2(5):285–297.
49. Garcia JA, et al. (2000) Impaired cued and contextual memory in NPAS2-deficient mice. *Science* 288(5474):2226–2230.
50. Sakai T, Tamura T, Kitamoto T, Kidokoro Y (2004) A clock gene, period, plays a key role in long-term memory formation in Drosophila. *Proc Natl Acad Sci USA* 101(45): 16058–16063.
51. Wardlaw SM, Phan TX, Saraf A, Chen X, Storm DR (2014) Genetic disruption of the core circadian clock impairs hippocampus-dependent memory. *Learn Mem* 21(8): 417–423.
52. Ouchi Y, et al. (2013) Reduced adult hippocampal neurogenesis and working memory deficits in the Dgcr8-deficient mouse model of 22q11.2 deletion-associated schizophrenia can be rescued by IGF2. *J Neurosci* 33(22):9408–9419.
53. Benedict C, et al. (2004) Intranasal insulin improves memory in humans. *Psychoneuroendocrinology* 29(10):1326–1334.
54. Cai Z, Fan L-W, Lin S, Pang Y, Rhodes PG (2011) Intranasal administration of insulin-like growth factor-1 protects against lipopolysaccharide-induced injury in the developing rat brain. *Neuroscience* 194:195–207.
55. Craft S, et al. (2012) Intranasal insulin therapy for Alzheimer disease and amnestic mild cognitive impairment: A pilot clinical trial. *Arch Neurol* 69(1):29–38.
56. Freiherr J, et al. (2013) Intranasal insulin as a treatment for Alzheimer's disease: A review of basic research and clinical evidence. *CNS Drugs* 27(7):505–514.
57. Reger MA, et al. (2008) Intranasal insulin administration dose-dependently modulates verbal memory and plasma amyloid-beta in memory-impaired older adults. *J Alzheimers Dis* 13(3):323–331.
58. Sun H, Lu B, Li RQ, Flavell RA, Taneja R (2001) Defective T cell activation and autoimmune disorder in Stra13-deficient mice. *Nat Immunol* 2(11):1040–1047.
59. Rossner MJ, Tirard M (2014) Thy1.2 driven expression of transgenic His_6-SUMO2 in the brain of mice alters a restricted set of genes. *Brain Res* 1575:1–11.
60. Brzózka MM, Radyushkin K, Wichert SP, Ehrenreich H, Rossner MJ (2010) Cognitive and sensorimotor gating impairments in transgenic mice overexpressing the schizophrenia susceptibility gene Tcf4 in the brain. *Biol Psychiatry* 68(1):33–40.